Stress Conditions in the Triaxial Compression Test

La Condition des Tensions dans l'Essai de Compression Triaxiale

by A. BALLA, Budapest, Hungary

Summary

The state of stress and strain in cylindrical specimens subjected to uniformly distributed axial and lateral forces is discussed. It introduces, on the basis of the theory of elasticity, a stress function in cylindrical coordinates valid for axially symmetrical stress distribution.

The stress and strain components deduced from the stress function satisfy the compatibility equation and the conditions of equilibrium.

Boundary conditions: (a) shearing stress acting along the lateral surface of the cylinder is equal to zero; (b) normal stress components in the radial direction on the lateral surface of the cylinder are constant; (c) the upper and lower boundary planes of the specimen remain plane throughout the deformation; and (d) the force acting on the top and bottom faces is equal to the sum of the stresses acting on the specimen.

In the equations appears a factor expressing the roughness of the loading-plate. Some numerical examples are considered.

In the final part, supposing the validity of the deduced stress-equations, the development of plastic regions, using the Huber-Mises theory of rupture, and the state of failure of the cylindrical specimen are analysed.

Sommaire

L'article discute la condition des tensions et des déplacements dans le cas des échantillons cylindriques soumis à des contraintes uniformes axiales et latérales. Il introduit, sur la base de la théorie d'élasticité, une fonction de tension valable pour la distribution des tensions axialement symmétriques.

Les composantes des tensions et des déplacements dérivées de la fonction des tensions répondent à l'équation de compatibilité et aux conditions d'équilibre. Les conditions limites sont les suivantes: (a) la tension de cisaillement employée sur la face est zéro; (b) la tension normale radiale sur la face est constante; (c) les bases du cylindre restent planes après la déformation; et (d) la force sur les bases est égale au total des tensions auxquelles l'échantillon est soumis.

Dans les équations paraît un facteur qui exprime la rugosité de la plaque de chargement. Exemples numériques.

Dans la dernière partie, l'auteur suppose, que la distribution trouvée à l'aide de l'élasticité, est valide et analyse le développement des régions plastiques d'après la théorie de rupture Huber-Mises et analyse l'état de rupture d'un échantillon cylindrique.

Theoretical Considerations

Introduction—The triaxial compression test aims at the determination of the shearing strength of soils. This testing method is becoming more familiar in laboratory practice, and the following question arises: what stresses and deformations occur at different points of the test specimen? It is the aim of this paper to answer the question.

The test specimen is cylindrical; the problem is treated in a cylindrical coordinate system on the basis of the theory of elasticity. The symbols used are shown in Fig. 1. As is known, in the case of axial symmetry, a stress function can be written down, and the stress and strain components derived therefrom satisfy the postulates of equilibrium and the deformation relations. This stress function satisfies the following differential equation:

$$\left(\frac{\partial^2}{\partial x^2}+\frac{\partial^2}{\partial r^2}+\frac{1}{r}\frac{\partial}{\partial r}\right)\left(\frac{\partial^2}{\partial x^2}+\frac{\partial^2}{\partial r^2}+\frac{1}{r}\frac{\partial}{\partial r}\right)\phi=\nabla^2\nabla^2\phi=0 \quad \ldots (1)$$

The stress equation—The above differential equation is satisfied by products of polynomials, sine and cosine functions, and of Bessel functions. The polynomials are of arbitrary degree, but certain relations must subsist between the coefficients in order to satisfy equation 1.

The differential equation has thus very many solutions. For the solution the simplest functions have been selected, so that the results are easy to handle and to evaluate numerically.

In the equation governing the stress function requirements of symmetry have already been satisfied.

The stress function used in the solution has the following form:

$$\phi=p_1\Big\{Cx^3+Dxr^2+Fx^5+Gx^3r^2+Kxr^4+$$

$$+\sum_{n=1}^{\infty}\left[A_nJ_0\left(i\frac{n\pi}{h}r\right)+B_nrJ_1\left(i\frac{n\pi}{h}r\right)\right]\sin\frac{n\pi}{h}x\Big\}+Lx^3p_2 \quad \ldots (2)$$

Determination of constants—The arbitrary constants have been determined from the following boundary conditions:

(1) Top and bottom surfaces of the cylinder remain plane after deformation and move parallel to their original position.

$$\xi_{x=h}=\nabla h \qquad \ldots . (3)$$

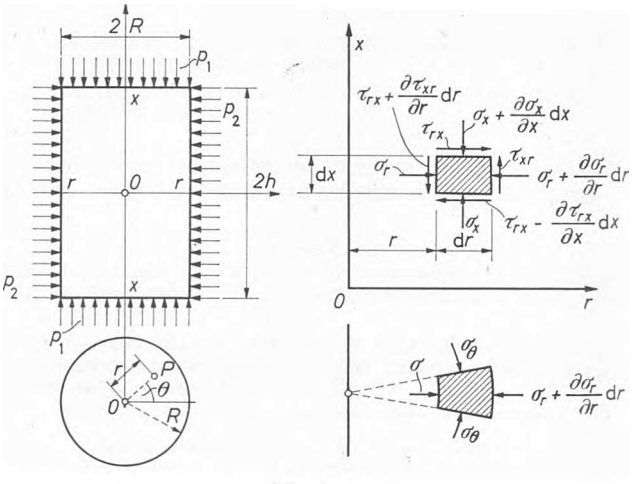

Fig. 1

(2) The horizontal radial stress σ_r is constant on the mantle surface

$$\sigma_{r=R}=p_2 \qquad \ldots . (4)$$

(3) The value of shearing stress on the mantle surface:

$$\tau_{r=R}=0 \qquad \ldots . (5)$$

(4) The external force acting on the loading surface and the

resultant of stresses transmitted by it are equal to each other; that is, equilibrium requires that

$$\int_0^{2\pi}\int_0^R \sigma_{x=h} r\,dr\,d\theta - R^2\pi p_1 = 0 \qquad \ldots. (6)$$

Consideration of the roughness of the loading surface—After the introduction of the above boundary conditions there remains one constant unknown. From the point of view of the soil mechanics experiment it is important to know whether the roughness of the loading surface has any effect on the results of the test. Therefore a coefficient characterizing the roughness of the loading plate is now introduced.

We consider a circular sector of angle $d\theta$. Then the ratio of the resultants of the shearing stresses and of the normal stresses acting upon the sector we define as proportional to the roughness f of the loading surface

$$f = \frac{d\theta\int_0^R \tau_{x=h} r\,dr}{d\theta\int_0^R \sigma_{x=h} r\,dr} \qquad \ldots. (7)$$

Stress and deformation components—The stresses and deformations have been derived from the stress function equation, and the values of the constants have been determined from the boundary conditions. Expressions for the stresses are given by the following equations:

$$\sigma_x = p_1 - p_1 f\left[\frac{24(1-\mu)x^2 + 12\mu r^2}{16(1-\mu)}\frac{1}{hR} - \frac{3}{\pi}\sum_{n=1}^{\infty} F_{\sigma x}\cos n\pi\frac{x}{h}\right] + p_1 f\frac{90\mu Qfp_1 + 32(7-2\mu+5\mu^2)\frac{h}{R}p_2}{15\mu.L.f.p_1 + 32(1-4\mu-5\mu^2)\frac{h}{R}p_2}\frac{L}{16(1-\mu)}\frac{R}{h} + \frac{1-\mu}{\mu}p_2 \qquad \ldots. (8)$$

$$\sigma_r = p_1 f\left[\frac{L}{16(1-\mu)}\frac{R}{h} + \frac{24x^2 - 3(3-2\mu)r^2}{16(1-\mu)}\frac{1}{hR} - \frac{3}{\pi}\sum_{n=1}^{\infty} F_{\sigma r}\cos n\pi\frac{x}{h}\right] + p_2 \qquad \ldots. (9)$$

$$\sigma_\theta = p_1 f\left[\frac{L}{16(1-\mu)}\frac{R}{h} + \frac{24x^2 - 3(1+2\mu)r^2}{16(1-\mu)}\frac{1}{hR} - \frac{3}{\pi}\sum_{n=1}^{\infty} F\sigma_\theta\cos n\pi\frac{x}{h}\right] + p_2 \qquad \ldots. (10)$$

$$\tau = p_1 f\left[\frac{3}{2}\frac{1}{hR}xr - \frac{3}{\pi}\sum_{n=1}^{\infty} F_\tau \sin n\pi\frac{x}{h}\right] \qquad \ldots. (11)$$

The following abbreviations are used in the above formulae

$$L = 3(3-2\mu) - 8\left(\frac{g}{R}\right)^2$$

$$Q = \mu + 4(1-\mu)\left(\frac{h}{R}\right)^2\left(1 - \frac{4}{\pi^2}\sum_{n=1}^{\infty}\frac{\cos^2 n\pi}{n^2}\right)$$

$$F_{\sigma x} = \Gamma_n\left\{\left[1 - 2(2-\mu)\frac{1}{n\pi}\frac{h}{R}U_n\right]J_0\left(i\frac{n\pi}{h}r\right) - U_n\frac{r}{R}\frac{1}{i}J_1\left(i\frac{n\pi}{h}r\right)\right\}$$

$$F_{\sigma r} = \Gamma_n\left\{\left[1 - (1-2\mu)\frac{1}{n\pi}\frac{h}{R}U_n\right]J_0\left(i\frac{n\pi}{h}r\right) - \left[\frac{h}{n\pi}\frac{1}{r} + U_n\frac{r}{R}\right]\frac{1}{i}J_1\left(i\frac{n\pi}{h}r\right)\right\}$$

$$F_{\sigma\theta} = \Gamma_n\left\{(2\mu-1)\frac{1}{n\pi}\frac{h}{R}U_n J_0\left(i\frac{n\pi}{h}r\right) + \frac{h}{n\pi}\frac{1}{r}\frac{1}{i}J_1\left(i\frac{n\pi}{h}r\right)\right\}$$

$$F_\tau = \Gamma_n\left\{\frac{r}{R}U_n J_0\left(i\frac{n\pi}{h}r\right) - \left[1 - 2(1-\mu)\frac{1}{n\pi}\frac{h}{R}U_n\right]\frac{1}{i}J_1\left(i\frac{n\pi}{h}r\right)\right\}$$

where

$$\Gamma_n = \frac{\cos n\pi}{\frac{1}{i}J_1\left(i\frac{n\pi}{h}R\right)V_n.n}$$

$$U_n = \frac{(3-\mu)\frac{1}{n\pi}\frac{h}{R} - (1-\mu)\frac{iJ_0\left(i\frac{n\pi}{h}R\right)}{J_1\left(i\frac{n\pi}{h}R\right)}}{(1-\mu)\left[\left(\frac{2}{n\pi}\right)^2\left(\frac{h}{R}\right)^2 - 1\right] + (1+3\mu-2\mu^2)\frac{1}{n\pi}\frac{h}{R}\frac{iJ_0\left(i\frac{n\pi}{h}R\right)}{J_1\left(i\frac{n\pi}{h}R\right)}}$$

$$V_n = 1 - U_n\left[2(1-\mu)\frac{1}{n\pi}\frac{h}{R}\right] + \frac{iJ_0\left(i\frac{n\pi}{h}R\right)}{J_1\left(i\frac{n\pi}{h}R\right)}$$

in which $J_0\left(i\frac{n\pi}{h}r\right)$ and $J_1\left(i\frac{n\pi}{h}r\right)$ are Bessel functions of imaginary argument.

Applications

Computation of the stress state for triaxial compression—For the numerical evaluation of formulae 8–11 the values of the functions F and $\sum_{n=1}^{\infty} F\cos n\pi\frac{x}{h}$ were tabulated and plotted in graphs.

From these the stresses and deformations arising in test specimens can be determined for any combination of vertical and lateral applied pressure.

For example, with a lateral pressure $p_2 = 0{\cdot}5$ kg/cm² two cases were considered associated with a vertical compressive stress $p_1 = 1{\cdot}0$ kg/cm² and then with $p_1 = 1{\cdot}5$ kg/cm². The results have been computed and tabulated in Table 1. As a basis for calculation we have taken a slenderness (height:diameter) ratio of 1·5, Poisson's ratio $\mu = \frac{1}{3}$ and the coefficient of roughness $f = 0{\cdot}3$.

As a practical application the problem of failure of the test specimen arose. The theory of failure of M. Huber–R. von Mises may be taken as a basis. According to this the material is in a plastic state when the reduced stress S is constant

$$S = \kappa \text{ (constant)}$$

where this reduced stress is defined in terms of the stress components by the equation

$$S = \sqrt{\tfrac{1}{6}[(\sigma_x - \sigma_r)^2 + (\sigma_r - \sigma_\theta)^2 + (\sigma_\theta - \sigma_x)^2] + \tau^2}$$

For example, for the case where $p_2 = 0{\cdot}5$ kg/cm² and $p_1 = 1{\cdot}0$ kg/cm² the value of the reduced stress has been computed (Fig. 2).

If the value of the constant κ characteristic of the material is known the plastic domains can be calculated for any loading case. It is to be emphasized that the application of this method involves a certain approximation: if plastic domains develop, the pressure re-distributions transmitted to the parts still in the elastic state are ignored.

Case of unconfined compression, the effect of the slenderness of the specimen upon compressive strength—If $p_2 = 0$ the case

Table 1

$p_2 = 0{\cdot}5$ kg/cm² $p_1 = 1{\cdot}0$ kg/cm²

x/h		r/R = 0	0·2	0·4	0·6	0·8	1·0
1·0	σ_x	− 0·118	− 0·112	− 0·104	− 0·076	+ 0·017	+ 0·699
	σ_r	+ 1·117	+ 1·104	+ 1·065	+ 0·995	+ 0·878	+ 0·500
	σ_θ	+ 1·17	+ 1·110	+ 1·089	+ 1·054	+ 1·012	+ 0·989
	τ	0	+ 0·300	+ 0·600	+ 0·900	+ 1·200	+ 1·500
0·8	σ_x	+ 0·081	+ 0·083	+ 0·088	+ 0·096	+ 0·092	+ 0·039
	σ_r	+ 0·787	+ 0·774	+ 0·737	+ 0·669	+ 0·567	+ 0·500
	σ_θ	+ 0·787	+ 0·780	+ 0·758	+ 0·720	+ 0·658	+ 0·551
	τ	0	+ 0·043	+ 0·080	+ 0·111	+ 0·107	0
0·6	σ_x	+ 0·154	+ 0·150	+ 0·140	+ 0·113	+ 0·049	− 0·086
	σ_r	+ 0·598	+ 0·591	+ 0·570	+ 0·539	+ 0·513	+ 0·500
	σ_θ	+ 0·598	+ 0·593	+ 0·578	+ 0·552	+ 0·518	+ 0·489
	τ	0	+ 0·007	+ 0·012	+ 0·012	+ 0·007	0
0·4	σ_x	+ 0·149	+ 0·143	+ 0·125	+ 0·092	+ 0·051	− 0·023
	σ_r	+ 0·516	+ 0·514	+ 0·509	+ 0·504	+ 0·501	+ 0·500
	σ_θ	+ 0·516	+ 0·513	+ 0·507	+ 0·497	+ 0·484	+ 0·470
	τ	0	− 0·007	− 0·014	− 0·021	− 0·019	0
0·2	σ_x	+ 0·127	+ 0·121	+ 0·104	+ 0·079	+ 0·053	+ 0·038
	σ_r	+ 0·489	+ 0·490	+ 0·492	+ 0·497	+ 0·499	+ 0·500
	σ_θ	+ 0·489	+ 0·488	+ 0·486	+ 0·484	+ 0·483	+ 0·482
	τ	0	− 0·006	− 0·011	− 0·014	− 0·012	0
0	σ_x	+ 0·117	+ 0·112	+ 0·097	+ 0·076	+ 0·055	+ 0·071
	σ_r	+ 0·484	+ 0·485	+ 0·489	+ 0·494	+ 0·498	+ 0·500
	σ_θ	+ 0·484	+ 0·484	+ 0·483	+ 0·483	+ 0·482	+ 0·485
	τ	0	0	0	0	0	0

$p_2 = 0{\cdot}5$ kg/cm² $p_1 = 1{\cdot}5$ kg/cm²

x/h		r/R = 0	0·2	0·4	0·6	0·8	1·0
1·0	σ_x	+ 0·347	+ 0·357	+ 0·367	+ 0·411	+ 0·550	+ 1·572
	σ_r	+ 1·117	+ 1·104	+ 1·065	+ 0·995	+ 0·878	+ 0·500
	σ_θ	+ 1·117	+ 1·110	+ 1·089	+ 1·054	+ 1·012	+ 0·989
	τ	0	+ 0·300	+ 0·600	+ 0·900	+ 1·200	+ 1·500
0·8	σ_x	+ 0·644	+ 0·650	+ 0·657	+ 0·670	+ 0·662	+ 0·582
	σ_r	+ 0·787	+ 0·774	+ 0·737	+ 0·669	+ 0·567	+ 0·500
	σ_θ	+ 0·787	+ 0·780	+ 0·758	+ 0·720	+ 0·658	+ 0·551
	τ	0	+ 0·043	+ 0·080	+ 0·111	+ 0·107	0
0·6	σ_x	+ 0·757	+ 0·705	+ 0·734	+ 0·694	+ 0·597	+ 0·395
	σ_r	+ 0·598	+ 0·591	+ 0·570	+ 0·539	+ 0·513	+ 0·500
	σ_θ	+ 0·598	+ 0·593	+ 0·578	+ 0·552	+ 0·518	+ 0·489
	τ	0	+ 0·007	+ 0·012	+ 0·012	+ 0·007	0
0·4	σ_x	+ 0·747	+ 0·739	+ 0·712	+ 0·662	+ 0·600	+ 0·492
	σ_r	+ 0·516	+ 0·514	+ 0·509	+ 0·504	+ 0·501	+ 0·500
	σ_θ	+ 0·516	+ 0·514	+ 0·507	+ 0·497	+ 0·484	+ 0·470
	τ	0	− 0·007	− 0·014	− 0·021	− 0·019	0
0·2	σ_x	+ 0·717	+ 0·707	+ 0·680	+ 0·644	+ 0·603	+ 0·582
	σ_r	+ 0·489	+ 0·490	+ 0·492	+ 0·497	+ 0·499	+ 0·500
	σ_θ	+ 0·489	+ 0·488	+ 0·486	+ 0·484	+ 0·483	+ 0·482
	τ	0	− 0·006	− 0·011	− 0·014	− 0·012	0
0	σ_x	+ 0·701	+ 0·692	+ 0·672	+ 0·637	+ 0·607	+ 0·632
	σ_r	+ 0·484	+ 0·485	+ 0·489	+ 0·494	+ 0·498	+ 0·500
	σ_θ	+ 0·484	+ 0·484	+ 0·483	+ 0·483	+ 0·482	+ 0·485
	τ	0	0	0	0	0	0

of unconfined compression is obtained. Expressions for the stresses are similar to those given by FILON.* Filon's method involves polynomials of higher degree, and therefore his formulae are more intricate than ours; nevertheless the numerical results are almost entirely identical. Filon does not make use of a coefficient of roughness.

* L. N. G. FILON (1902). On the elastic equilibrium of circular cylinders under certain practical systems of load. *Phil. Trans. A*, **198**, 147.

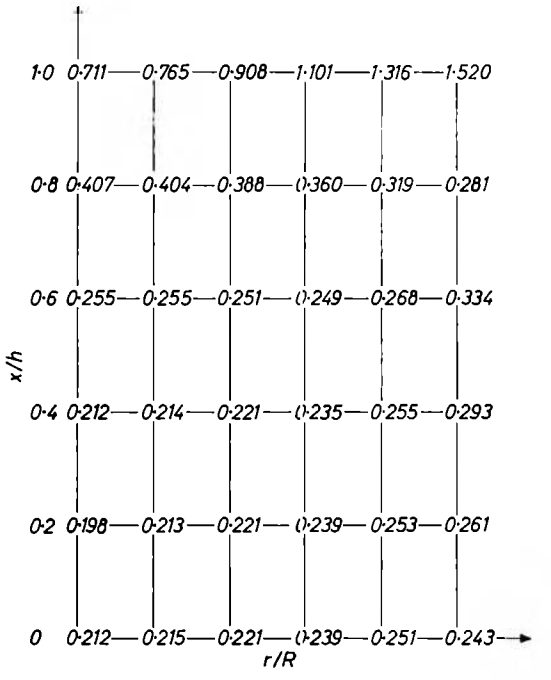

Fig. 2

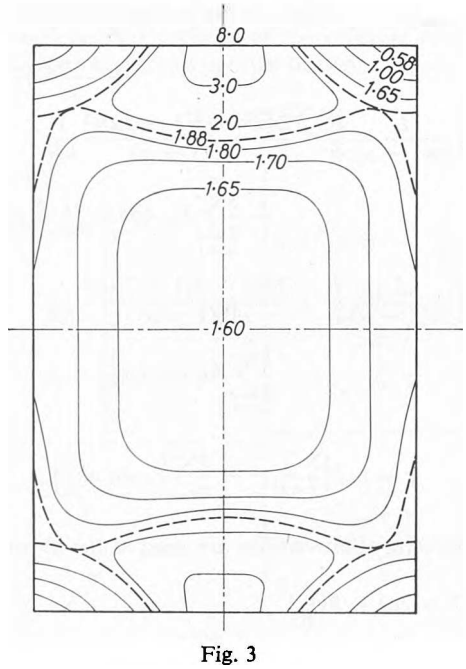

Fig. 3

The problem of failure may be investigated by the application of the concept of reduced stress. In this case the vertical stress may be taken from under the radical sign:

$$S = p_1\sqrt{k}$$

In the case of failure:

$$S = p_1\sqrt{k} = \kappa$$

$$p_1 = \frac{1}{\sqrt{k}}\kappa$$

where κ is a characteristic of the soil, and the value of k may be computed for any point of the test specimen. In this way—with the approximation mentioned in the previous section—the magnitude of the external load at which the plastic state arises at individual points of the specimen may be found. The test specimen fails when the plastic domains developing from the

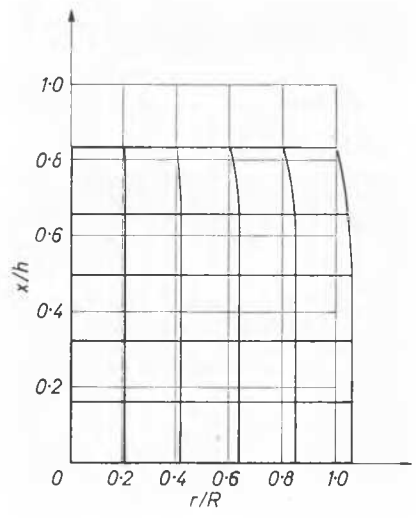

Fig. 4

boundary and from the centre meet. A numerical example is given in Fig. 3.

The problem was investigated for different slenderness ratios of the test specimen. It was found that the value of the compressive strength decreased with the increase of the slenderness ratio of the test specimen.

Problems of deformation—The deformation of the test specimen can also be obtained. For the case of unconfined compression it was computed, and the deformations are plotted in Fig. 4.

Effect of the roughness of the loading plate—As evidenced by the formulae, the roughness of the loading plate affects the values of the stresses and of the deformations.

The case of the unconfined compression test where $f = 0$ was considered; that is, the loading plate was supposed perfectly frictionless. For this case it was found that

$$\sigma_x/p_0 = 1, \quad \sigma_r/p_0 = 0, \quad \sigma_\theta/p_0 = 0, \quad \tau/p_0 = 0; \quad S = 0,$$
$$S = 0{\cdot}577p_0$$

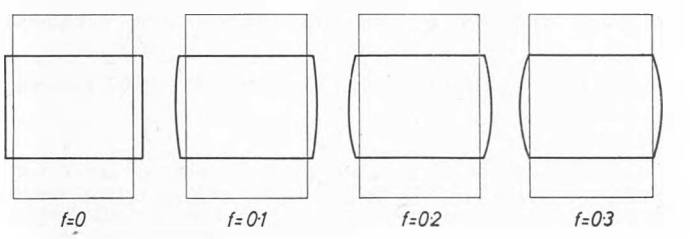

Fig. 5

That is a vertical stress equal to the external loading acts at every point of the specimen, the other stresses being equal to zero.

As for deformations it was found that horizontal plane sections of the body remained plane after deformation and were displaced parallel to their original positions.

The effect of roughness on deformations was further investigated—again for the case of unconfined compression—and it was observed that, as shown above, in the case $f = 0$ the test specimen became a cylinder, shorter but of increased diameter. Further, for increasing roughness it assumes more and more a barrel form, with maximum bulge in the middle. The character of the deformation is shown in Fig. 5.